

CHAPTER 83

WAVE SPECTRA TRANSFORMATIONS

Giancarlo Chiaia, Leonardo Damiani, Antonio Petrillo *

Abstract

In this paper the transformations of sea waves, reproduced by a JONSWAP spectrum in a laboratory channel, have been studied both in frequency and time domain. In frequency domain the occurrence of non-linearities producing energy transfers to high and low frequencies was studied. The reported experimental results enabled us to compare the two approaches and to define the limits within which they give the same results.

INTRODUCTION

The transformations of a sea state when moving from deep to shallow waters can be studied by analyzing how the values of its characteristic quantities vary in the time as well as in the frequency domain.

Although describing the same physical phenomenon, these two approaches are not always equivalent and often give quite different results, especially when great transformations have already occurred.

The study of the correlation between the results of the two methods is particularly important both for setting up and applying mathematical models to foresee the pattern of spectral shapes, as well as for application purposes, such as the estimate of the significant wave height for the design of sea works. Moreover, the knowledge of local sea states is indispensable for the study of solid transportation.

In this work the two types of analyses were made, referring to one-dimensional JONSWAP spectra generated in a wave channel with a sand bar-shaped bed, in order to define their applicability limits. We analyzed the occurrence of non-linearities by introducing first Ursell number and then a

*Hydraulics and Hydraulic Constructions Institute
Bari University - Via ReDavid, 200 - BARI (ITALY)

dimensionless depth and by establishing the limits of linear propagation (Thompson and Vincent, 1985).

Some singularities observed in the pattern of parameters calculated in the frequency domain led us to study the energy components at low frequencies, especially near the shore. These were studied according to the theory of reflection of small amplitude waves, which, despite the approximation due to the non-linearity of the problem, enabled us to identify the presence of an almost standing component (surf-beat) with remarkable energy quantities in the surf-zone.

Finally, the analysis in the time domain enabled us to establish the limits within which the knowledge of the energy spectrum can be applied to estimate the quantities of interest to engineers.

DESCRIPTION OF EXPERIMENTAL SET-UP AND FACILITIES

Experiments were carried out in the wave channel at the laboratory of the Hydraulics and Hydraulic Constructions Institute of Bari University.

The channel is about 45 m long and 1 m wide; its walls consist of 1.2 m high crystal glass sheets supported by iron frames with a center to center distance of about 0.44 m, resulting in 100 gauging cross-sections along the whole length of the channel (the 100th cross-section coincides with the wave generator paddle location). The channel bottom is covered with a sand layer of a pretty uniform size $d_{50}=0.15$ mm and with a corresponding fall velocity $\omega = 0.018$ m/s. Experiments are also being carried out to assess the performance of some submerged breakwaters (Lamberti et al., 1985); therefore, at a distance of 4.5m from the wave generator, the channel has been longitudinally subdivided into two parts in order to simulate the evolution of an unprotected beach, in one part, and the evolution of a protected beach under the same wave attack in the other. The experimental measurements reported in this paper were all made in the former. Two bars, whose crests were approximately located at cross-sections 60 and 30, were observed in the channel during the tests.

The wave generation system consists of a flat paddle which receives a rotatory-translational motion: the kinematic mechanism which drives the paddle is designed for the axis of rotation to be lower than the channel bottom, this being a better condition to generate waves at shallow depths. The paddle is set in motion by an oleo-dynamic system driven by an electrical valve which, through an electrical signal, sends pressurized oil to the two ends of the cylinder in which the piston moves. The piston displacements, measured by a transducer, control the system in a closed chain circuit and give it a good stability in the applied field of frequencies. The whole system is controlled by a processing computer.

The small water losses occurring in the channel, especially between the paddle and the channel walls, are compensated by an automatic supply system driven by an electrical water gauge equipped with a band-pass filter which eliminates wave-generated surface oscillations. During the tests, the water depth near the paddle was 0.8 m with level fluctuations of about 0.1 mm.

In Froude undistorted similarity with 1:10 length scale, the tests reproduce some meteomarine conditions of mid-Adriatic sea (Italy).

The sea states in the channel were represented by energy density JONSWAP spectra with amplification parameter $\gamma=3.3$ and shape factor $\omega=0.07$ for $f < f_p$ and $\omega=0.09$ for $f > f_p$. The wave attacks tested in the channel have off-shore significant heights (H_s) ranging from 8.34 to 24.17 cm and significant period (T_s) ranging from 1.49 to 2.13 s, corresponding to JONSWAP spectra with peak frequencies in the range $(0.44-0.63 \text{ s}^{-1})$ and zero-th order moments m_0 of the spectra varying from 5 to 42 cm^2 .

In this study we analyzed the results referring to five wave attacks of the same peak frequency (0.507 s^{-1}) and m_0 (evaluated at the first monitoring cross-section) ranging between 5.20 and 36 cm^2 . For these attacks measurements are available at all the gauge stations of the channel, this being indispensable to describe a complete wave pattern.

The measurements in the channel were made through capacitive probes, calibrated before each experiment and connected to a processing computer through an analogue-digital converter. For each measurement the data acquisition was made simultaneously with three probes, for a time of 102,4 s and a sampling interval of 0.1 s. The three probes were also used to assess the incident and reflected spectra (Lamberti et al., 1986).

The probes could measure the wave state up to cross-section 8, since the low water depth near the shoreline makes the measurements poorly reliable because of the presence of air mixed with water.

Telecamera shots were used to measure the wave flow also in the area between cross-sections 8 and 5, where the swash-zone starts (Damiani and Ranieri, 1989), and to check the data obtained from the probes between cross-sections 13 and 8 where the presence of air bubbles can invalidate the probe measurements. The frame by frame shot enabled to have the time pattern of the free water level fluctuations.

The data taken by the probes or the telecamera were processed both in the time (up-zero-crossing method) and the frequency domain.

In the latter case, the n-th order spectral density moments were calculated through numerical integration; hence the average spectral periods ($T_{01} = m_0/m_1$ and $T_{02} = \sqrt{(m_0/m_2)}$) as well as the parameters of spectral width ($\epsilon_2 = (m_0 m_2/m_1^2 - 1)^{0.5}$ and $\epsilon_4 = (1 - m_2^2/(m_0 m_4))^{0.5}$) were obtained.

Through partial integration of the spectrum the energy content in the neighbourhood of the peak frequency and its two first harmonics (E_1, E_2, E_3) were calculated assuming, in agreement with other authors (Guza and Thornton, 1980), $0.9n f_p$ and $1.1n f_p$ with $n=1, 2, 3$ as integration limits.

The equivalent and significant wave heights $H_{rms} = \sqrt{8m_0}$ and $H_s = 4\sqrt{m_0}$ were calculated for an infinitely narrow spectrum.

For the study of low frequency waves (among which the surf-beat) the energy and the height H_{rms} of the examined frequencies were also calculated by integrating the spectrum on a $3\delta f$ large band, centered on the concerned frequency, with δf being the resolution frequency of the spectrum.

By applying the up-zero-crossing method for each cross-section all the statistical characteristics of the wave state were calculated. The water level rise distribution was also analyzed with respect of Gauss distribution by applying χ^2 test and calculating the skewness and the the kurtosis ($\beta_1, \sqrt{\beta_2}$).

The definitions and symbols of quantities were taken from the "List of Sea State Parameters" (I.A.H.R., 1987).

ANALYSIS OF EXPERIMENTAL RESULTS

Linear Propagation Field

In figure 1 the configuration of the sand bed of the channel with the two previously mentioned bars is illustrated. It also shows the energy spectra measured at some representative cross-sections and referred to a wave attack of a peak frequency equal to $0.507 s^{-1}$ and a zero-th order moment of the spectrum equal to

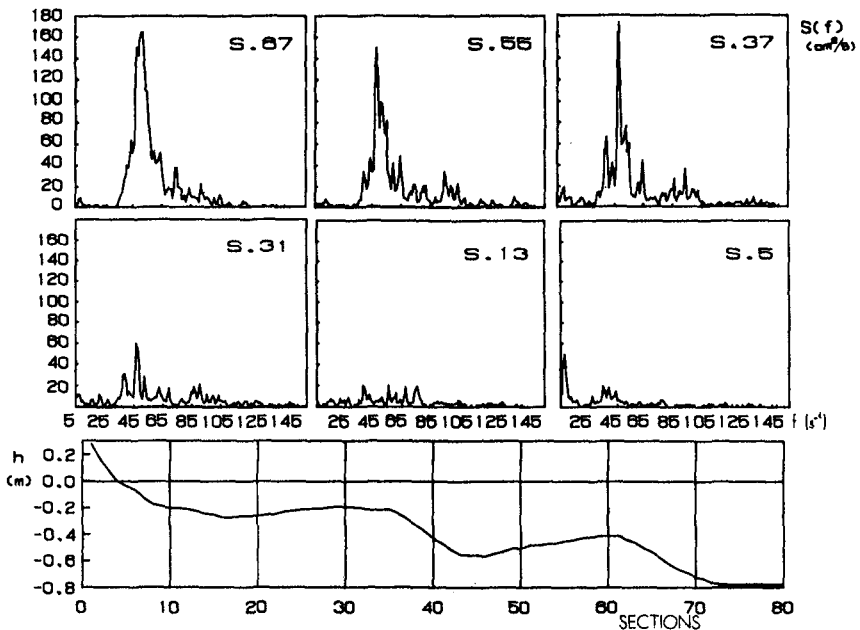


Figure 1. Beach profile and sample of spectra assessed in different cross-sections.

$28 cm^2$ at the first gauging cross-section.

This figure emphasizes the transformations of the spectrum in its propagation up to the shoreline. Already in the zone off-shore the first bar, where only shoaling is present (cross-section 67), the spectrum transformations result in an energy transfer to high frequencies; afterwards, flowing over the off-shore bar,

it is noticed a first wave breaking, which produces a decline of the energy content at the peak frequency and an increase of the above said transfers. It then follows a recomposition phase in which the energy content at peak frequency grows up and energy quantities at low frequencies start being remarkable. The high energy dissipations, due to the wave breaking on the on-shore bar, cause a remarkable flattening of the spectrum at cross-section 31. The spectrum completely changes its initial shape at cross-section 13, so that it is no longer possible to detect any energy content at the peak frequency. Near the shoreline (cross-section 5) the only significant energy content is the one at low frequency (surf-beat): this points out that very slow oscillations of the mean sea level occur in this area.

Definitely, moving from off-shore to the shoreline, waves basically undergo three kinds of transformations: energy transfers towards high frequencies, breaking dissipations and energy transfers towards low frequencies. The energy transfer towards high frequencies shows that non-linearities occur in the propagation of spectra.

The non-linearities were studied by analyzing the ratios of the energy quantities around the first and the second harmonic to the peak frequency energy (Guza and Thornton, 1980; Petrillo, 1988). These ratios were taken as a function of Ursell number calculated through $Ur = H_{rms} L_p^2 / h^3$, where h is the local depth and L_p is the local wave length at the peak frequency (Figure 2).

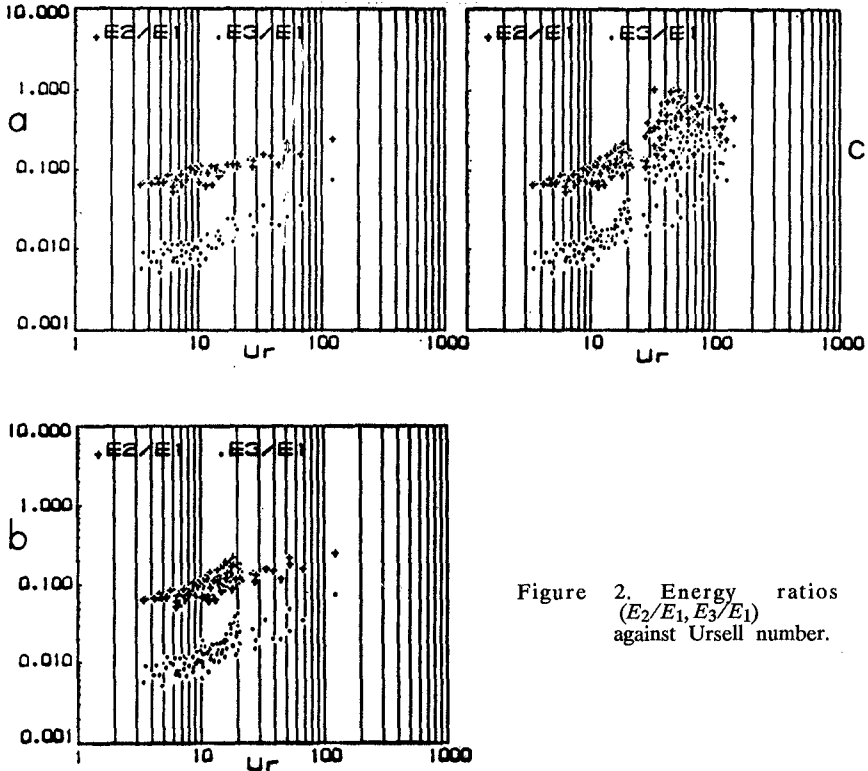


Figure 2. Energy ratios ($E_2/E_1, E_3/E_1$) against Ursell number.

In order to emphasize the shoaling, the breaking and the bar-effects, the pattern of these ratios was studied by plotting first the data off-shore the first bar (i.e. before breaking) (figure 2.a), then those before the on-shore bar (including the previous ones, but always excluding data of cross-sections where waves break) (figure 2.b) and, at last, the values of the ratios for all the cross-sections, including those of breaking (figure 2.c).

By comparing figures 2.a and 2.b it is noticed that the presence of bars locally creates some non-linearities. When flowing over the on-shore bar, wave breaking occurs and non linearities increase as shown in the figure 2.c.

From the analysis of the enclosed and examined diagrammes, considering that for a theoretical JONSWAP spectrum with $\gamma=3.3$ the E_2/E_1 and E_3/E_1 ratios are respectively equal to 0.083 and 0.008, it can be stated that the non-linearities on the first harmonic appear when Ursell number values are higher than 6, whereas the non-linearities on the second harmonic appear at higher Ur values (about $Ur > 10$). These results are in agreement with those found by Guza and Thornton (1980) and other authors.

Instead of Ursell number, the dimensionless depth $K_{p0}h$ (where $K_{p0}=2\pi/L_0$ is the wave number, calculated by referring to the peak frequency), which is easier to determine, can be applied to study the occurrence of non linearities at high frequencies.

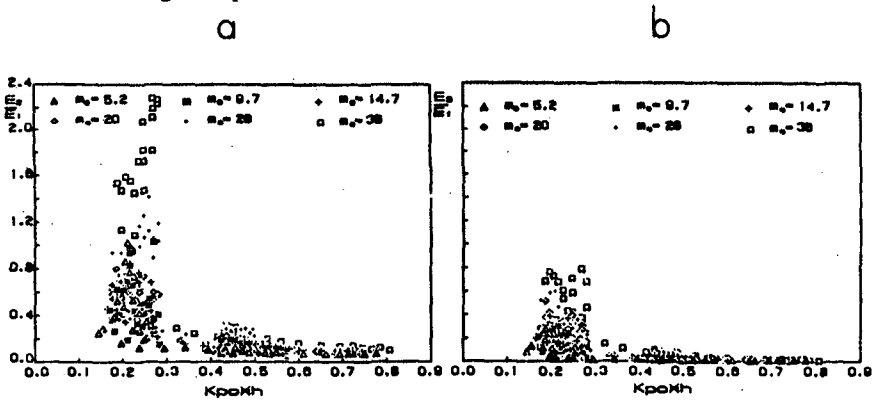


Figure 3. Energy ratios ($E_2/E_1, E_3/E_1$) versus $K_{p0}h$.

From the analysis of figure 3, reporting the data for all the gauging cross-sections and all the wave attacks, it is shown that non-linearities occur both on the first and the second harmonic when $K_{p0}h$ is greater than 0.8.

It has to be observed that, since the examined attacks have all the same peak frequency, and so the same L_p , and since the non-linearity depends on the H/h and h/L_p ratios (Petrillo, 1988), h being equal, non-linearities increase with the increase in energy of the wave attack.

The pattern of ϵ_2 , and ϵ_4 as a function of Ursell number is reported in figure 4; for values of $Ur < 6$, the two parameters have values quite close to those

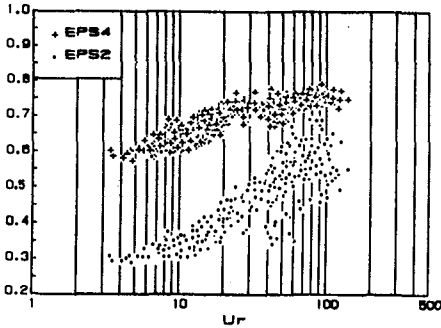


Figure 4. Spectral width parameter (narrowness parameter and broadness factor) against Ursell number.

of the undistorted JONSWAP spectrum ($\epsilon_2=0.329$ and $\epsilon_4=0.658$); they increase with the increase of Ursell number in a way qualitatively similar to that of the E_2/E_1 and E_3/E_1 ratios; the same behaviour is observed for ϵ_2 and ϵ_4 as a function of $K_p h$.

Figure 4 also shows that ϵ_2 , which has higher relative variations, is more significant than ϵ_4 in representing the phenomenon; this is in agreement with Thornton and Guza (1983).

Analysis in the Frequency Domain

Referring to the wave attack with $m_o=36\text{ cm}^2$, figure 5 illustrates the pattern of H_{rms} calculated on the basis of the energy content of the whole spectrum and then of the spectrum around the surf-beat frequency (0.0781 s^{-1}); the figure also reports the pattern of the $T_{0.2}/T_p$ and $T_{0.1}/T_p$ ratios and the beach profile.

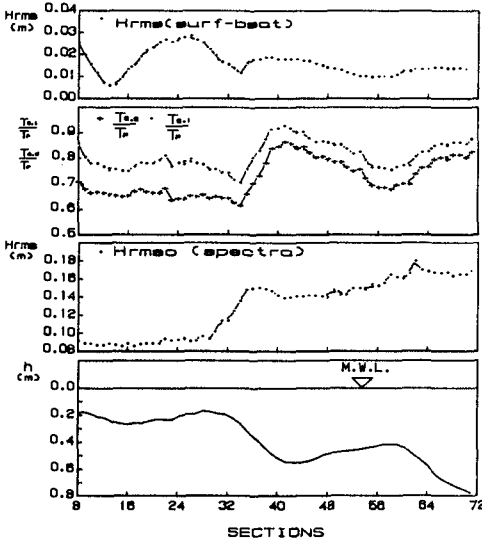


Figure 5. Beach profile; H_{rms} , $T_{0.2}/T_p$, $T_{0.1}/T_p$ values, assessed across the shore.

The pattern of H_{rms} of the whole spectrum is indicative of the kind of transformations which spectrum undergoes when approaching the shoreline: shoaling until reaching the off-shore bar; small wave breaking on the bar; then recomposition; shoaling again up to the on-shore bar; large wave breaking on it and, at last, spectrum reaches the shoreline with a saturated energy content in the wind-wave band.

The mean spectral periods decrease in the shoaling area and on the bar because of the energy contents increase on the second and the third harmonic; during recomposition, periods increase, go back to normal values, then they decrease again because of shoaling on the

on-shore bar and, at last, they become minimum in the area of highest wave breaking. Downstream of the on-shore bar (see figure 1), the spectrum is flat and so the values of average periods remain basically constant. Nevertheless the

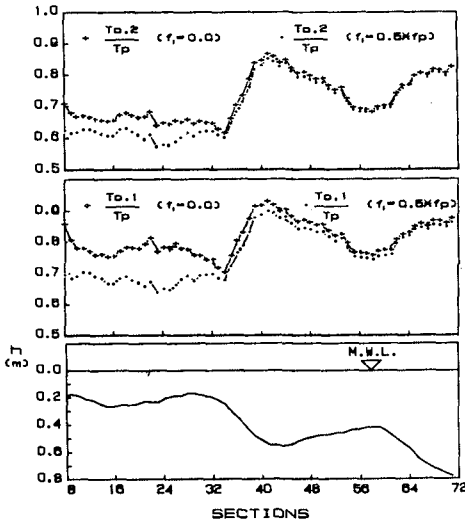


Figure 6. Dimensionless mean spectral periods H_{rms} , $T_{0.2}/T_p$, $T_{0.1}/T_p$ across the shore, evaluated with different integral limits in n-th order moments calculation.

pattern of mean periods in this area shows an increase in the proximity of cross-sections 22 and 8 where the surf-beat energy values are maximum.

The influence of surf-beat at the cross-sections downstream of the on-shore bar on the the first and second order moments, and then on the mean spectral periods, can be observed in figure 6 which also illustrates the pattern of the mean spectral periods, calculated by integrating the spectrum starting from the frequencies $f_1=0$ and $f_1=0.5f_p$. It is noticed that the two quantities are the same up to the cross-section of maximum wave breaking (cross-section 34), whereas they greatly differ downstream the on-shore bar, where the surf-beat energy is greater. In this area the value of the $T_{0.2}/T_p$ ratio fluctuates, for the considered wave attack, in the range 0.62–0.67, and it decreases (about 10%) if the contribution due to low frequencies is omitted. Near

the shoreline, where the surf-beat reaches its absolute maximum value, such a ratio becomes equal to 0.72 and it reduces (15%) if the surf-beat contribution is omitted. The same pattern is observed for the parameter $T_{0.1}/T_p$.

The mean spectral periods, for all the examined wave attacks, are plotted in figures 7a and 7b, as a function of $k_p h$. It is noticed that for $k_p h > 0.6$, independently of the energy of attacks, the dimensionless periods remain rather constant ($T_{0.1}/T_p = 0.87$ and $T_{0.2}/T_p = 0.846$). These values are slightly different

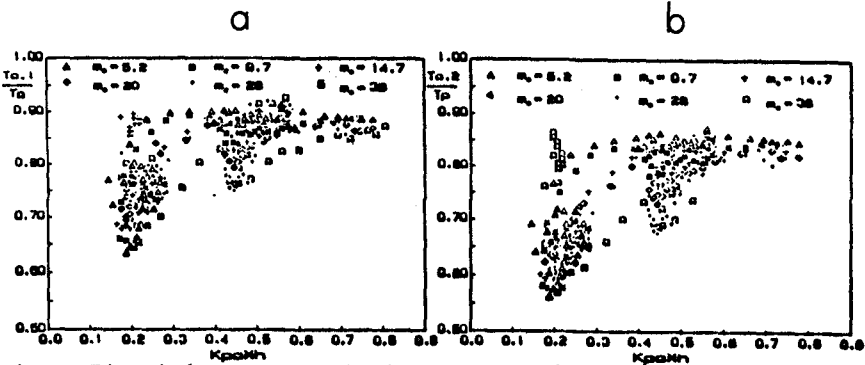


Figure 7. Dimensionless mean spectral periods versus $K_p h$ for all the wave attacks.

from the theoretical ones of JONSWAP spectrum with $\gamma=3.3$, respectively equal to 0.844 and 0.801. These deviations, (3% for $T_{0.1}/T_p$ and 6% for $T_{0.2}/T_p$) are to be attributed to the inevitable errors produced in spectrum generation and survey. Nevertheless, the previous figures show the same trend found by other authors (Bendykowska, 1986; Liberatore and Petii, 1988).

For $K_{po}h > 0.6$, on the average, $T_{0.2}/T_p$ and $T_{0.1}/T_p$ tend to decrease with $k_{po}h$, but, differently from the results by other authors (Bendykowska, 1986), who found a monotone and always decreasing pattern, in the present experiments a high variability was observed as a function of the wave energy.

This behaviour is clearly linked to the non-linearities which occur during propagation (shoaling, bars, wave breaking) and to low frequency standing waves, both related to the wave energy and to the shape of the beach profile.

In order to show that surf-beat is really a standing wave produced by reflection from the beach, the small amplitude wave theory was applied (in spite of the approximations due to the non-linearity of the phenomenon). According this theory the resulting wave amplitude should be enveloped by the curves representing respectively the sum and the difference between the incoming and reflected waves. Figure 8 illustrates, for some frequencies, the heights of the resulting monochromatic waves, the sum of the incoming and reflected waves heights and their difference, along the channel. The above mentioned heights have been calculated by integrating around the considered frequency, respectively the spectrum surveied in the cross sections and the incoming and reflected spectra, assessed through the three probe method.

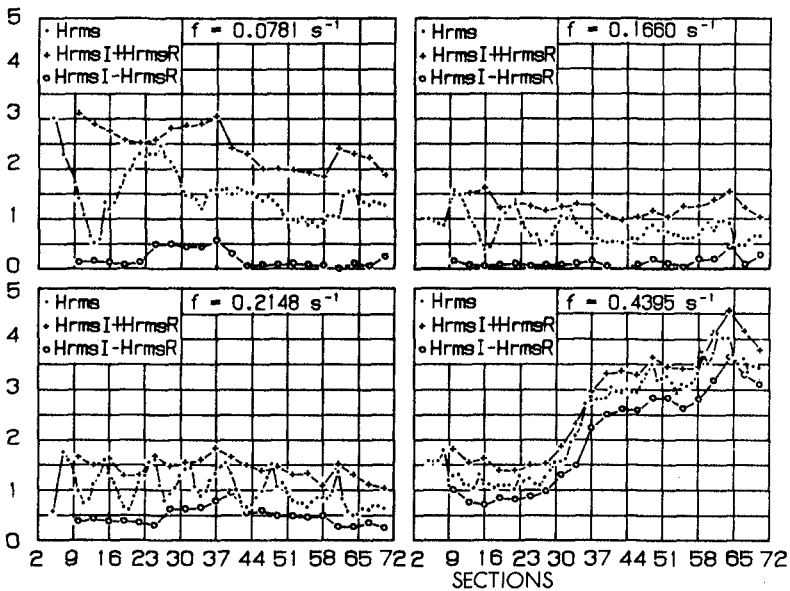


Figure 8. Envelope of monochromatic components according to small amplitude wave theory.

It can be observed that surf-beat component (at the frequency $0.0781s^{-1}$ in model scale) is a quasi pure standing wave because the progressive component (represented by the difference between the incoming and reflected waves) is very little if compared with the standing one (difference between the two lines representing the sum of the incoming and reflected wave heights and their difference): that means an almost complete reflection from the beach at the surf-beat frequency.

For the monochromatic components with frequencies higher than the surf-beat one, the progressive component is larger, but a standing component is still present: that means a partial reflection; the reflection lessens with frequency increasing and it becomes negligible near the peak frequency where monochromatic components can be represented by pure progressive waves.

Analysis in the Time Domain

The patterns of T_s/T_p and T_z/T_p (with T_s and T_z , respectively significant and average periods, both assessed in the time domain) for the attack with $m_o=36 cm^2$ and $f_p=0.507 s^{-1}$, as well as the beach profile are illustrated in figure 9.

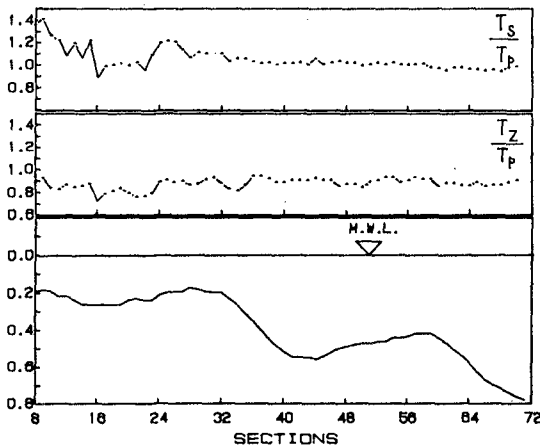


Figure 9. Dimensionless wave periods (T_s/T_p and T_z/T_p), evaluated in time domain, across the shore.

In agreement with the results by other authors (Liberatore and Petti, 1988) T_z/T_p is not so much affected, at least up to the on-shore bar, by the transformations of the spectrum when passing from higher to lower depths. This ratio ranges around 0.9, higher than the theoretical value referred to JONSWAP spectrum with $\gamma=3.3$; such a difference is similar to the one observed in the analysis of the mean periods in frequency domain. The T_s/T_p ratio is, on the average, equal to 1.00 up to the on-shore bar, with a slightly decreasing trend. This enables to refer to the peak frequency of the

spectrum, rather than to the significant one, when using the models for studying the wave transformations. This is always true far from breaking; after breaking the T_s/T_p ratio is sensitive to the distortions of the spectrum, especially near the shoreline, where it is also affected by low frequency standing waves and the dimensionless significant period reaches the value 1.40.

Figures 10.a and 10.b report dimensionless wave periods, for all the examined wave attacks, as a function of $K_p h$. The two figures show quite the same behaviour.

For $K_p h > 0.6$, T_s/T_p is almost constant, with an average value equal to 0.975, whereas for $0.3 < K_p h < 0.6$, a dispersion of experimental data is observed with a slightly decreasing pattern. For values of $K_p h < 0.3$, the behaviour of different wave attacks greatly differs: the significant period increases with the increase of the attack energy and, hence, of the surf-beat it produces. In this area the data referring to the attacks with $m_o = 5; 10; 15 \text{ cm}^2$ fall below the straight line representative of the mean value off-shore, whereas, for higher energy, they fall above. These results are in agreement with those reported in figure 3. The same conclusions may be drawn from the analysis of the behaviour of T_s/T_p as a function of Ursell number: it is constant for $Ur < 10$; for $10 < Ur < 30$ the data are scattered around the mean value despite the presence of a band of variability; whereas for $Ur > 30$ the points form a cloud with increasing T_s/T_p values for the wave attacks of higher energy.

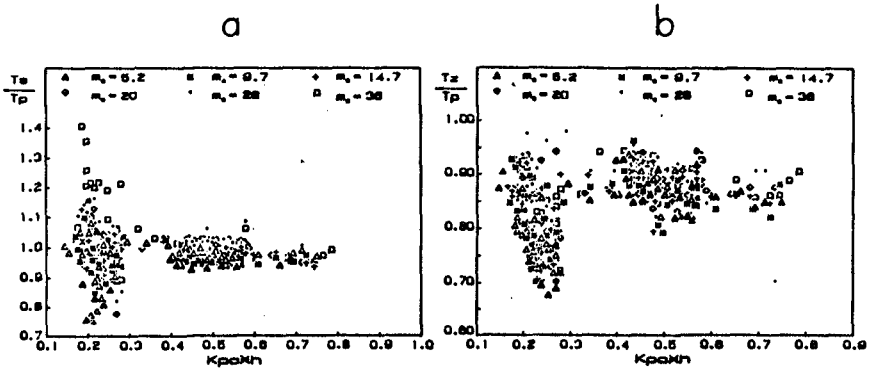


Figure 10. Dimensionless periods, evaluated in time domain, versus $K_p h$ for all waves attacks.

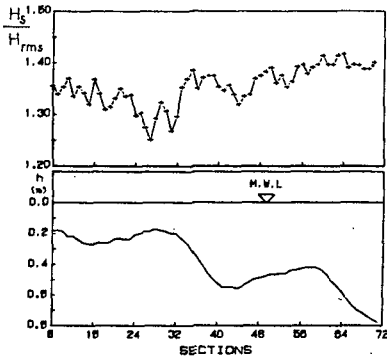


Figure 11. Beach profile and H_s/H_{rms} across the shore.

For the previously examined attack, figure 11 reports the pattern of H_s/H_{rms} ratio, calculated in the time domain. It is noticed that, except at some cross-sections, H_s/H_{rms} is not greatly influenced by the wave transformations: it decreases from 1.40 to 1.34 from off-shore to the shoreline, with lower values between cross-sections 24 and 32, where it reaches the minimum value 1.25. These results are partly in agreement with those found by Thornton and Guza (1983). In their experiments on gentle slope beaches, they found that the ratio H_s/H_{rms} is constant and equal to 1.42 for a sea state following wave heights Rayleigh distribution.

Figure 12 reports the ratio between the wave energy calculated in the time domain ($E_{td} = 1/8 \rho g H_{rms}^2$) and the energy assessed by integration of the spectrum (given by $E_{fd} = \rho g m_o$) and the skewness and kurtosis of elevations along the shore.

The figure shows that at the cross-sections off-shore the first bar, where the spectrum is not markedly affected by non-linearities, both the skewness and the kurtosis have values close to those of Gauss distribution and E_{td}/E_{fd} approaches to 1, that is the time and frequency domain analyses give the same results.

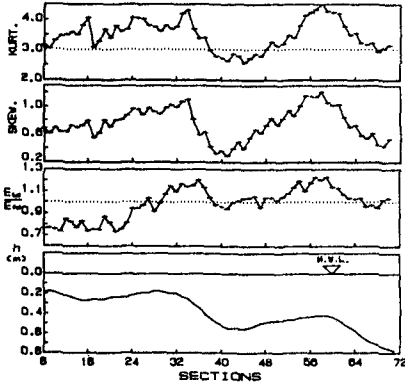


Figure 12. Beach profile, time domain energy rated to frequency domain energy, Skewness, and Kurtosis of surface elevations.

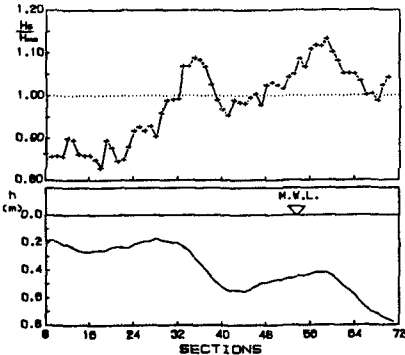


Figure 13. Comparison between significant wave height values calculated in the time domain and through the zero-th order moment of the spectrum.

When the spectrum is affected by non-linearities (produced by shoaling, bar-effect and breaking), both the kurtosis and the skewness increase: the former because of decreasing of maximum wave heights and hence of a greater probability around the average value, the latter because of energy transfers at high frequencies which makes the waves similar to cnoidal waves. In this case E_{td}/E_{fd} increases and reaches the maximum value of about 1.2.

In the inner surf-zone, the strong dissipations due to wave breaking produce a notable flattening of the spectrum, thus, as it is reported by other authors (Dally and Dean, 1988), the H_{rms} height, calculated in the time domain, declines and the E_{td}/E_{fd} ratio becomes lower than 1. Finally, from the figure it can be stated that the assumption $H_{rms} = \sqrt{8}m_o$, which links a quantity calculated in the time domain to a quantity obtained in the frequency domain, can be applied only when the non-linearities are far away. This is partly in disagreement with the results by other authors (Thornton and Guza, 1983), who noticed that the above said relationship can be applied also in the case of breaking waves.

Figure 13 illustrates the ratio between the significant height, H_s , calculated by the up-zero-crossing method and the significant height, H_{smo} , obtained from the spectrum which, in the case of JONSWAP spectrum with $\gamma=3.3$, is related to the zero-th order moment through the relationship $H_{smo} = 3.866\sqrt{m_o}$.

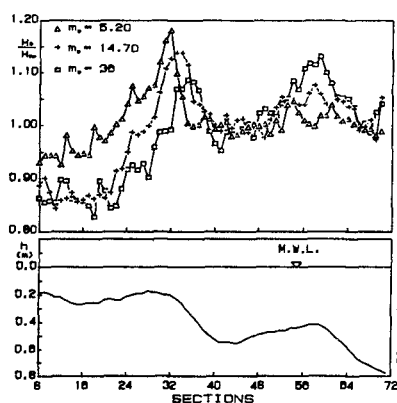


Figure 14. Behaviour of (H_s/H_{smo}) ratio for different wave attacks.

This ratio has a pattern qualitatively similar to that of E_{id}/E_{fd} illustrated in figure 12.

The pattern of H_s/H_{smo} , for three wave attacks of different energy (figure 14), shows that the deviations of the ratio from 1 depend on the attack energy. This is in agreement with the results found by Thompson and Vincent (1985) who relate the deviations of H_s/H_{smo} to the local steepness, which is a strictly increasing function of the energy for each cross section, since all the described wave attacks have the same peak frequency.

CONCLUSIONS

The analysis of the experimental results, confirms how difficult it is to establish a direct correlation between the characteristic quantities of a wave state in the frequency and in the time domain.

In fact, the results from the two types of analysis are well correlated only in a limited field of linear propagation with values of the parameter $k_p h > 0.6$, or $Ur < 10$.

Out of this field, the evaluation of the characteristic quantities in the time domain based on the knowledge of those in the frequency domain, entails big errors in that the spectrum, because of the great non-linearities occurring during propagation, can no longer represent the physical phenomenon correctly; in these zones it is better to refer to the time domain.

It was shown that, for values of $k_p h < 0.3$, a decreasing trend of the mean spectral periods $T_{0.1}$ and $T_{0.2}$ was observed, due to the presence in this zone of low frequency standing waves which greatly affect them, whereas the characteristic periods in time domain (T_s and T_c) are less affected by non-linearities.

Following on the lack of direct correlation of the results from the two methods, it is difficult to evaluate the significant wave height (needed to design sea structures) based on the knowledge of the spectrum.

The analysis in frequency domain pointed out some monochromatic components at low frequencies and, among them, the surf-beat ($f=0.0781s^{-1}$ in model scale) with a great energy content in the surf-zone and a maximum value near the coast. Some authors (Bredshaw, 1980) assumed that the genesis of the phenomenon is related to the fact that, after breaking, the wave recomposes and generates new bigger waves which capture and incorporate smaller ones. This mechanism should produce a gradual change in the spectrum, passing from the

breaking point to the shoreline, in that going towards shallow waters a gradual absorption of smaller waves is supposed to occur. The present experiments, although not showing such a gradual absorption, showed, in the surf-zone, the presence of energy quantities at frequencies between the surf-beat and the peak one. It is thought, however, that although the above-said mechanism may contribute to the energy transfer to low frequencies, the presence of surf-beat is essentially due to the reflection of the beach (*Guza and Thornton, 1985*) which generates a standing wave at low frequency.

References

- Bendykowska, G., Spectral characteristics of irregular waves over sloping bottom, Atti del XX Convegno di Idraulica e Costruzioni Idrauliche, Padova, 1986.
- Bredshaw, M.P., Topographic control of run-up variability, Proc. 17th Intern. Coast. Eng. Conf., 1980.
- Dally, R.W., G.R. Dean, Closed-form solutions for the probability density of wave height in the surf-zone, Proc. 21th Intern. Coast. Eng. Conf., 1988.
- Damiani, L., M. Ranieri, Oscillazioni sottocosta prodotte da onde random, Atti del II Congresso A.I.O.M., Napoli, 1989.
- Goda, Y., Statistical variability of sea parameters as a function of wave spectrum, XXII Conf. I.A.H.R., Seminar Maritime Hydraulics section, 1987.
- Guza, R.T., E.B. Thornton, Local and shoaled comparisons of sea surface elevations, pressures and velocities, J. of Geophys. Res., Vol. 85, 1980.
- Guza, R.T., E.B. Thornton, Observations of surf beat, J. of Geophys. Res., Vol. 90, 1985.
- International Association for Hydraulics Research List of Sea State Parameters, XXII Conf. I.A.H.R., Lausanne, 1987.
- Lamberti, A., A. Petrillo, M. Ranieri, A comparative analysis of some types of submerged barriers as beach defense structure, XXI Conf. I.A.H.R., 1985.
- Lamberti, A., A. Petrillo, M. Ranieri, Generation of irregular waves in an experimental channel, V Conf. Asian and Pacific Reg. Div. I.A.H.R., 1986.
- Liberatore, G., M. Petti, Modification of random waves characteristics in shoaling waters, Excerpta, Vol. 3, 1988.
- Petrillo, A., Evoluzione delle onde di mare su bassi fondali sabbiosi con pendenza variabile, IX Congr. A.I.M.E.T.A., Bari, 1988.
- Thompson, E.F., C.L. Vincent, Significant wave height for shallow water design, J. of Waterway, Port, Coastal and Ocean Eng., Vol.3, 1985.
- Thornton, E.B., R.T. Guza, Transformation of wave height distribution, J. of Geophys. Res., Vol. 88, 1983.

